



Journal Name

COMMUNICATION

Nonaqueous synthesis of metal cyanamide semiconductor nanocrystals for photocatalytic water oxidation

Received 00th January 20xx,
Accepted 00th January 20xxWei Zhao,^a Jie Pan^{a, b} and Fuqiang Huang *^{a, c}

DOI: 10.1039/x0xx00000x

www.rsc.org/

Herein, we report nonaqueous synthesis of metal cyanamide semiconductor nanocrystals, including Ag₂NCN nanorods (NRs), ZnNCN NRs and PbNCN nanoparticles. The as-prepared Ag₂NCN NRs with band gap of 2.35 eV are applied as photocatalysts for water oxidation. The oxygen evolution rate (280.7 μmol h⁻¹g⁻¹) is much higher than that of Ag₂NCN microcrystals (24.0 μmol h⁻¹g⁻¹).

Colloidal semiconductor nanocrystals (NCs) have attracted great interest during the last two decades since the successful synthesis of monodisperse cadmium chalcogenide nanocrystals in 1993.^{1, 2} Their fascinating properties such as tunable size, shape and composition and modulated band gap and optical absorption and emission endow semiconductor nanocrystals with potential applications in diverse fields.³ Recently, metal carbodiimide or cyanamide (MNCN, M = Mn, Fe, Co, Ni, Cu, Zn, etc.), as an important type of metal pseudochalcogenide, is growing up as novel functional material.^{4, 5} Because of oxygen-like behaviour of NCN group and large electron negativity of the terminal nitrogen atoms, intriguing physicochemical properties and promising technological applications can be anticipated when substituting O²⁻ anion in metal oxide with NCN²⁻ anion.^{6, 7} For example, phase-pure Cr₂(NCN)₃ is demonstrated as ferromagnet compared with its antiferromagnetic oxide counterpart (Chromium(III) oxide, Cr₂O₃), opening the way for seeking new magnetic materials.⁸ Eu²⁺ doped SrNCN is regarded as a promising candidate for luminescent material host.⁹ Bulk MNCN (M = Fe, Co, Ni, Mn) crystals are successfully applied as anode materials for Lithium/sodium ion batteries, exhibiting excellent cycling performance.^{10, 11} Ag₂NCN microcrystals (MCs) show degradation performance in

photocatalysis for waste water cleaning.¹² Whether charge storage performance or photocatalytic property is highly related to the specific surface area of the active materials.^{13, 14} Unfortunately, metal cyanamides are often prepared under high temperature, suffering from large crystal size and low surface area.¹⁵⁻¹⁷ It is highly demanded to obtain metal cyanamide nanocrystals with high surface-to-bulk ratio to increase the surface area.¹⁸ Additionally, considering the size dependent properties of colloidal semiconductor nanocrystals, if metal cyanamides can be acquired on nanometer-scale, fascinating properties and novel applications can be expected. In our previous paper, Ag₂NCN nanoparticles with high surface area were prepared in aqueous solution, however the size distribution is hard to control.¹² Alternatively, nonaqueous synthesis assisted by long chain organic molecules such as oleylamine (OMA), oleic acid (OA) should be a better choice because crystal size, morphology and dispersity can be effectively controlled by strong complexing capacity of organic surfactants.^{1, 2}

In this communication, we deliver a general strategy to synthesize metal cyanamide nanocrystals in nonaqueous solution by room temperature injection method. Ag₂NCN nanorods (NRs), ZnNCN NRs and PbNCN nanoparticles (NPs) are successfully prepared. In this protocol, primary amines are used as complexing agents and toluene/ethanol miscible solvents serve as reaction media. Take the synthesis of single crystalline Ag₂NCN NRs as example, the length and diameter of the nanorod was tuned by using different primary amines as chelating agents. The as-prepared Ag₂NCN NRs possess band gap energy about 2.35 eV, which can harvest visible light photons up to ca. 528 nm. As a proof-of-concept application, Ag₂NCN NRs are used as photocatalysts for water oxidation under visible light illumination and enhanced performance is obtained compared with that of the Ag₂NCN MCs precipitated in aqueous solution.

Colloidal synthesis of metal cyanamide nanocrystals was conducted in nonaqueous solution at room temperature. In this approach, primary amines dissolved in toluene were used as complexing agents for metal salt dissolution. When

^a State Key Laboratory of High Performance Ceramics and Super fine Microstructure, Shanghai Institute of Ceramics, Chinese Academy of Sciences, Shanghai 200050. Email: huangfq@mail.sic.ac.cn

^b University of Chinese Academy of Sciences, Beijing 100049, China.

^c State Key Laboratory of Rare Earth Materials Chemistry and Applications, College of Chemistry and Molecular Engineering, Peking University, Beijing 100871, P.R. China.

Electronic Supplementary Information (ESI) available: [details of any supplementary information available should be included here]. See DOI: 10.1039/x0xx00000x

cyanamide (H_2NCN) ethanol solution dropped into the toluene solution, precipitation reaction proceeded rapidly leading to the formation of metal cyanamide nanocrystals capped with surfactant molecules. In a typical synthesis of Ag_2NCN NRs, 1 mmol of AgNO_3 was dissolved in toluene, assisted with 1 mL of OMA. After stirring for 30 min, 1 M of H_2NCN ethanol solution (1 mL) was injected. The mixture solution was kept at room temperature to allow the growth of NRs, followed by centrifugation and purification.

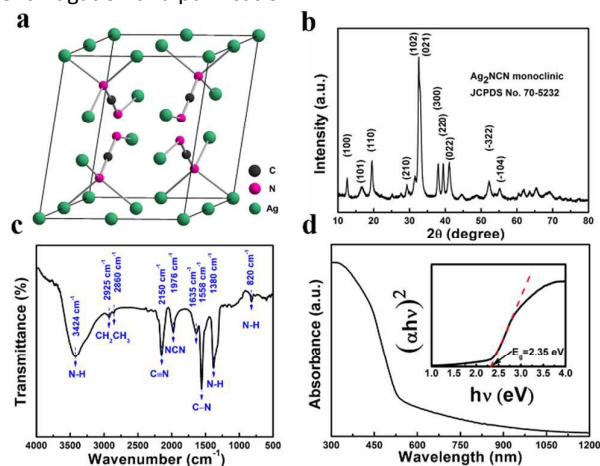


Figure 1. (a) Crystal structure of Ag_2NCN . (b-d) XRD pattern, FTIR spectrum and Ultraviolet-visible diffusive reflectance spectrum of the as-prepared Ag_2NCN sample with oleylamine as the capping agent. Inset in d shows the plots of $(\alpha h\nu)^2$ versus the energy of the exciting light.

Figure 1b shows the X-ray diffraction (XRD) pattern of the obtained Ag_2NCN NRs. All the diffraction peaks are indexed to the monoclinic Ag_2NCN (crystal structure shown in Figure 1a) with lattice constants of $a = 7.3147 \text{ \AA}$, $b = 6.0096 \text{ \AA}$, $c = 6.6839 \text{ \AA}$, $\beta = 102.2930^\circ$ (JCPDS No. 70-5232) and no any impurity phase is detected.¹⁹ The surface structure of the Ag_2NCN NRs was then investigated by Fourier transform infrared spectrum (FTIR) shown in Figure 1d. The characteristic peak at 1976 cm^{-1} reveals the existence of $[\text{NCN}]^{2-}$ anion. The peaks belonging to capped agents distribute in two areas: the bands between 1300 cm^{-1} and 1700 cm^{-1} are ascribed to the -NH scissoring mode and C-N stretching mode; the bands within the range of $2800\text{--}3000 \text{ cm}^{-1}$ are from the $-\text{CH}_2\text{CH}_3$ stretching vibrations. Whereas the slight shifts of some peaks, compared with that of the samples obtained in the aqueous solution (Figure S1d), may be due to the interaction between primary amines complexing agents and NRs. Above FTIR analysis suggests that OMA was indeed bound onto the NRs. The UV-Vis diffuse reflectance spectrum (Figure 1d) indicates that the as-prepared Ag_2NCN NRs can absorb solar energy with a wavelength shorter than $\sim 528 \text{ nm}$. This absorption characteristics without absorption peaks resembles with that of Ag_2NCN MCs we reported before.¹² A direct band gap (E_g) of 2.35 eV is derived from the absorption spectrum (inset in Figure 1d), a little higher than the theoretical value.

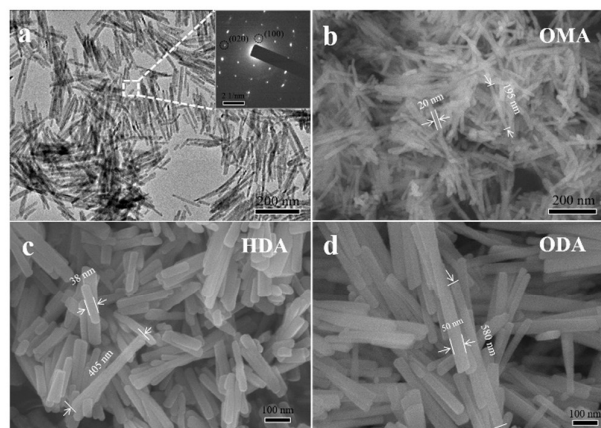


Figure 2. (a, b) Low-resolution TEM and FESEM images of the Ag_2NCN NRs obtained in toluene with oleylamine (OMA) as the capping agent, inset in (a) displays the SAED pattern of an individual nanorod. (c, d) FESEM images of the as-prepared Ag_2NCN NRs using hexadecylamine (HDA) and octadecylamine (ODA) as capping agents. The typical size of an individual nanorod is marked in the images.

Figure 2a displays a representative transmission electron microscope (TEM) image of the as-prepared Ag_2NCN NRs. When OMA is used as capping agent for AgNO_3 dissolution, Ag_2NCN NRs with average length of 200 nm and diameter of 20 nm can be prepared. Each NR is single-crystalline, evidenced by the bright selected area electron diffraction (SAED) pattern of an individual NR (inset in Figure 1a). The nanorod morphology is also confirmed by the field emission scanning electron microscope (FESEM) (Figure 1b) where the size and shape is agreeable with TEM characterization. The possible growth mechanism of the NRs was investigated by monitoring the change of morphology, phase purity and absorption spectra of the samples along with the reaction time (Detailed illustration can be found in the SI, Figure S2, S3). According to the TEM, XRD and optical property measurements, the generation of NRs may obey a diffusion-controlled growth mechanism.²⁰ In order to clarify the effect of capping agents on the morphology of the samples, another two primary amines with different chain length including hexadecylamine (HDA) and octadecylamine (ODA) are also used in the reaction media. Likewise, Ag_2NCN NRs can be obtained, whose typical diameter and length are about 38 nm and 405 nm for HDA directed sample (Figure 2c). As for ODA, the length and diameter of the sample are 50 nm and 580 nm, respectively. Obviously, the length and diameter of the obtained NRs are successfully tuned, which could be ascribed to the different complexing capacity of the primary amines. The selected three primary amines have different pK_b (OMA : 3.34; HDA : 3.37; ODA : 3.41). Because of a lower value of pK_b , OMA is a stronger base and capping with Ag^+ more tightly to facilitate preferential growth, leading to smaller nanorod diameter compared with HDA and ODA. In the other hand, if no primary amine was added, Ag^+ could not dissolve in toluene. If primary amines were replaced by primary acids,

such as OA, only irregular particles were obtained maybe due to the weak coordination between Ag^+ and OA in toluene. Therefore, primary amines play a pivotal role in the synthesis of Ag_2NCN NRs. The strong complexing ability makes the nonaqueous reaction in a homogeneous solution and structure-directing effect results in a regular morphology.²¹ The obtained oil-soluble NRs can be well dispersed in nonpolar solvent and converted into water-soluble NRs by ligand exchange treatment.²²

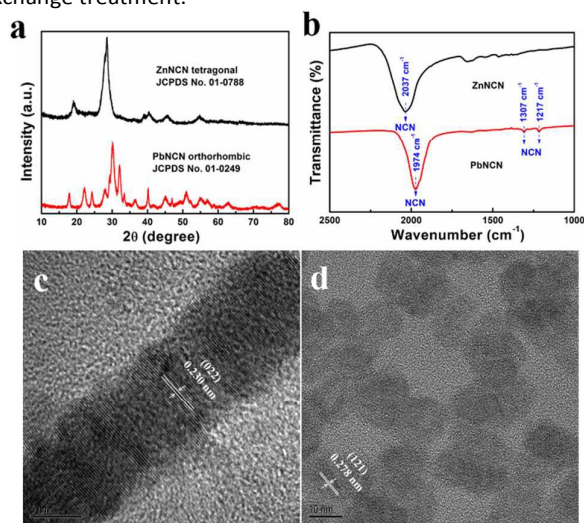


Figure 3. (a) XRD patterns, (b) FTIR spectra and (c, d) TEM images of the ZnNCN NRs and PbNCN NPs synthesized with oleylamine as the capping agent.

Since the synthesis of Ag_2NCN NRs is conducted by a one-pot precipitation reaction between AgNO_3 and H_2NCN , high yield production is expected. In fact, when 1 mmol (170 mg) of AgNO_3 is used as silver source, 118 mg of Ag_2NCN NRs can be prepared, meaning a yield of 93 % with respect to AgNO_3 . The small loss may be originated from the multiple washing process. In one batch, we can prepare 12 g of Ag_2NCN NRs (Figure S4) with an enlarged reaction container using 0.1 mol of AgNO_3 . Therefore, this approach provides us a facile and environment-friendly method for gram-scale production of Ag_2NCN NRs. Besides Ag_2NCN NRs, ZnNCN NRs and PbNCN NPs can be also synthesized when AgNO_3 is replaced by other metal salts such as ZnCl_2 and PbCl_2 after selecting appropriate capping agents. Their crystal structures are examined by XRD (Figure 3a) and can be indexed to tetragonal ZnNCN (JCPDS No. 70-4898) and orthorhombic PbNCN (JCPDS No. 72-1116), respectively. The typical peaks at 1974 cm^{-1} and 2037 cm^{-1} in FTIR spectra (Figure 3b) confirm the existence of $[\text{NCN}]^{2-}$ anion in the as-prepared nanocrystals. Compared the IR spectra of these two samples with Ag_2NCN NRs, more peaks can be found in Ag_2NCN NRs, PbNCN NPs, but less in ZnNCN NRs. Such a difference should be due to the existence of two electronic forms of $[\text{NCN}]^{2-}$ anion. The symmetric carbodiimide $[\text{N}=\text{C}=\text{N}]^{2-}$ form in ZnNCN and the asymmetrical cyanamide $[\text{N}\equiv\text{C}-\text{N}]^{2-}$ form in PbNCN, while they were proposed to coexist in the $[\text{NCN}]^{2-}$ anion of Ag_2NCN .²³ The measured absorption spectra

(Figure S5) indicate that ZnNCN NRs can only absorb UV light while PbNCN NPs can harvest visible light. TEM images shown in Figure 3c-d and Figure S6 show length and diameter about 90 nm and 8 nm for ZnNCN NRs and particle size about 10 nm for PbNCN NPs. All the above characterization results demonstrate the successful synthesis of Ag_2NCN , PbNCN and ZnNCN nanocrystals and the proposed procedure is a universal route toward the synthesis of metal cyanamide semiconductor nanocrystals.

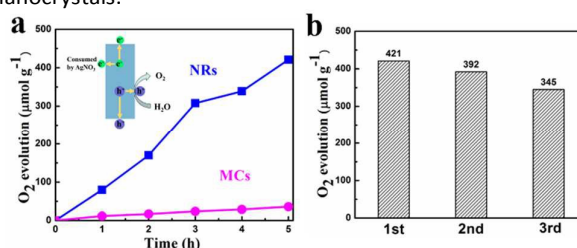


Figure 4. (a) Comparison of the photocatalytic O_2 evolution rates using Ag_2NCN NRs and MCs as the active materials, inset shows the process of visible-light driven water splitting by NRs with AgNO_3 as the sacrificial agent. (b) Recycling test of the NRs for O_2 evolution.

From the measured absorption spectra above, Ag_2NCN NRs can capture visible light. In our previous paper, the band edge position of Ag_2NCN was already confirmed by electrochemical method, whose CBM and VBM is calculated at about 0.15 eV and 2.43 eV (vs. NHE), respectively.¹² Compared with the redox potential of $\text{O}_2/\text{H}_2\text{O}$ (1.23 V), Ag_2NCN should be capable for water oxidation under visible-light irradiation. In the photo-response loop of Ag_2NCN , the photo-carriers were proposed to be generated by exciting electrons from N 2p to Ag 5s orbital ($\text{N } 2p^6 \text{ Ag } 4d^{10} 5s^0 \rightarrow \text{N } 2p^5 \text{ Ag } 4d^{10} 5s^1$).¹² After bond rearrangement of $[\text{NCN}]$ group, the released free holes on N sites may be used to facilitate photocatalytic oxygen evolution. In order to confirm this prediction, photocatalytic water splitting for O_2 evolution is conducted from aqueous solution containing AgNO_3 as a sacrificial agent. After visible-light irradiation ($\lambda \geq 420\text{ nm}$), the photoexcited electron-hole pairs were created and separated, followed by hole induced water oxidation and electron consumed by AgNO_3 (Inset in Figure 4a). The rate of evolved O_2 reached ca. $280.7\text{ }\mu\text{mol h}^{-1}\text{g}^{-1}$ over Ag_2NCN NRs without using any co-catalyst, while only $24.0\text{ }\mu\text{mol h}^{-1}\text{g}^{-1}$ of O_2 was generated over the Ag_2NCN MCs under the same condition (Figure 4a). The former one is nearly 11-fold higher than that of the latter one, indicating a higher photocatalytic activity of Ag_2NCN NRs. Oxygen evolution rate of the as-prepared Ag_2NCN NRs is also compared with the reported data of other semiconductors such as Ag_3PO_4 , C_3N_4 , Bi_2WO_6 , and BiVO_4 , listed in Table S1. As novel type photocatalysts for O_2 production, the performance of Ag_2NCN NRs is not comparable to the top-performance photocatalysts Ag_3PO_4 and BiVO_4 , but superior to that of C_3N_4 and Bi_2WO_6 .

Generally, the light harvesting and specific surface area have great influence on the photocatalytic performance. According to the absorption spectra (Figure 1d and Figure S1d), the band gap energies of Ag_2NCN NRs and MCs are close to each other

(2.35 eV vs. 2.32 eV). Higher surface area can provide more active sites for catalytic reaction. The measured specific surface areas are $28.20 \text{ m}^2 \text{ g}^{-1}$ and $2.86 \text{ m}^2 \text{ g}^{-1}$ for Ag_2NCN NRs and MCs, respectively (Figure S7). The oxygen evolution rates normalized to surface area are $9.81 \mu\text{mol h}^{-1} \text{m}^{-2}$ and $8.39 \mu\text{mol h}^{-1} \text{m}^{-2}$ for NRs and MCs, respectively, indicating the superior performance of NRs. Herein, besides absorption property and surface area effect, the superior performance of Ag_2NCN NRs compared with MCs could be attributed to the efficient separation of excited electron-hole pairs and prompt transport of charge carriers. The single-crystalline nature of NRs can facilitate unidirectional charge transport along the NR axial direction.²⁴ Additionally, small lateral size of NRs can short the distance for carrier migration to surface and benefit transfer and separation of excited electron-hole pairs, resulting an enhanced photocatalytic activity (inset in Figure 4a). After three successive runs, the generated O_2 was $345 \mu\text{mol g}^{-1}$, keeping 82.0 % activity of the first run (Figure 4b). The degraded performance may be due to the declined crystallinity and partial decomposition of NRs after recycling tests, which was uncovered by comparison of the XPS spectra, XRD patterns and absorption spectra of the Ag_2NCN NRs before and after photocatalytic test (Figure S8). The emergence of metallic Ag particles coated on the photocatalyst surface may inhibit the light absorption of the catalysts and also decrease the amounts of active materials, resulting in reduced performance. To expand the potential applicability, the photocatalytic activity towards organic dye (MB, MO, and RhB) degradation under visible-light irradiation was also investigated, further demonstrating the superior performance of Ag_2NCN NRs compared with MCs (Figure S9, S10).

In our previous paper, we reported Ag_2NCN was a visible-light active photocatalyst for organic contaminant decomposition.¹² In this study, we discover that Ag_2NCN MCs are less active toward water oxidation maybe due to the strong recombination of photoexcited electron-hole pairs in bulk form. In order to solve this problem and improve the photocatalytic activity, morphology control in nonaqueous solution is a vital step. Our prepared Ag_2NCN NRs display better performance for water photooxidation. The enhanced activity can be attributed to the higher specific surface area and single-crystalline nature of the NRs. Tuning Ag_2NCN from inert to active by morphology control is an encouraging achievement, which is also found in brookite TiO_2 single-crystalline nanosheet.²⁵

In summary, we develop a general method to synthesis metal cyanamide semiconductor nanocrystals in nonaqueous solution. The as-prepared Ag_2NCN NRs with band gap energy about 2.35 eV are demonstrated with excellent performance for photocatalytic water oxidation and organic dye degradation under visible-light irradiation. The achievements demonstrate that metal cyanamide semiconductor nanocrystals can be obtained by colloidal synthesis in organic solution. The outstanding photocatalytic performance of Ag_2NCN NRs shed light on the application of metal cyanamide nanocrystals for solar energy utilization.

The authors acknowledge the Financial support from the National Key Research and Development Program (Grant No. 2016YFB0901600), NSF of China (Grants 61376056, 51672301 and 51672295).

Notes and references

1. C. Murray, D. J. Norris and M. G. Bawendi, *J Am Chem Soc*, 1993, **115**, 8706-8715.
2. Y. Yin and A. P. Alivisatos, *Nature*, 2005, **437**, 664-670.
3. D. V. Talapin, J.-S. Lee, M. V. Kovalenko and E. V. Shevchenko, *Chemical Reviews*, 2010, **110**, 389-458.
4. R. Riedel, E. Kroke, A. Greiner, A. O. Gabriel, L. Ruwisch, J. Nicolich and P. Kroll, *Chem Mater*, 1998, **10**, 2964-2979.
5. A. Zorko, P. Jeglic, A. Potocnik, D. Arcon, A. Balcytis, Z. Jaglicic, X. Liu, A. L. Tchougreeff and R. Dronskowski, *Phys Rev Lett*, 2011, **107**.
6. T. D. Boyko, R. J. Green, R. Dronskowski and A. Moewes, *J Phys Chem C*, 2013, **117**, 12754-12761.
7. D. Ressnig, M. Shalom, J. Patscheider, R. More, F. Evangelisti, M. Antonietti and G. R. Patzke, *J Mater Chem A*, 2015, **3**, 5072-5082.
8. R. Dronskowski, X. J. Tang, H. P. Xiang, X. H. Liu and M. Speldrich, *Angew Chem Int Edit*, 2010, **49**, 4738-4742.
9. R. Dronskowski, M. Krings, G. Montana and C. Wickleder, *Chem Mater*, 2011, **23**, 1694-1699.
10. A. Eguia-Barrio, E. Castillo-Martinez, X. Liu, R. Dronskowski, M. Armand and T. Rojo, *J Mater Chem A*, 2016, **4**, 1608-1611.
11. M. T. Sougrati, A. Darwiche, X. H. Liu, A. Mahmoud, R. P. Hermann, S. Jouen, L. Monconduit, R. Dronskowski and L. Stievano, *Angew Chem Int Edit*, 2016, **55**, 5090-5095.
12. W. Zhao, Y. F. Liu, J. J. Liu, P. Chen, I. W. Chen, F. Q. Huang and J. H. Lin, *J Mater Chem A*, 2013, **1**, 7942-7948.
13. T. Hisatomi, J. Kubota and K. Domen, *Chemical Society Reviews*, 2014, **43**, 7520-7535.
14. N. Mahmood, T. Tang and Y. Hou, *Advanced Energy Materials*, 2016, **6**, n/a-n/a.
15. R. Dronskowski, X. H. Liu, M. Krott, P. Muller, C. H. Hu and H. Lueken, *Inorg Chem*, 2005, **44**, 3001-3003.
16. R. Dronskowski, X. H. Liu, L. Stork, M. Speldrich and H. Lueken, *Chem-Eur J*, 2009, **15**, 1558-1561.
17. R. Dronskowski, M. Krings, M. Wessel, W. Wilsmann and P. Muller, *Inorg Chem*, 2010, **49**, 2267-2272.
18. D. Koziej, F. Krumeich, R. Nesper and M. Niederberger, *J Mater Chem*, 2009, **19**, 5122-5124.
19. M. Becker, J. Nuss and M. Jansen, *Z. NATURFORSCH. B*, 2000, **55**, 383-385.
20. M. Kruszynska, *ACS Nano*, 2012, **6**, 5889-5896.
21. T.-D. Nguyen, *Nanoscale*, 2013, **5**, 9455-9482.
22. A. Nag, M. V. Kovalenko, J.-S. Lee, W. Liu, B. Spokoyny and D. V. Talapin, *J Am Chem Soc*, 2011, **133**, 10612-10620.
23. X. Liu, *PhD thesis*, University of Aachen, Germany, 2002.
24. B. Liu and E. Aydil, *J Am Chem Soc*, 2009, **131**, 3985-3990.
25. H. Lin, L. Li, M. Zhao, X. Huang, X. Chen, G. Li and R. Yu, *J Am Chem Soc*, 2012, **134**, 8328-8331.